# Separate Reconstruction of Speed of Sound, Density, and Absorption Parameters in Ultrasound Inverse Scattering Tomography

*Sung-Jae Kwon

※ This work was supported by the Daejin University Research Grants in 1998.


## Abstract

This paper proposes a method of separately determining three intrinsic mechanical parameters of an unknown object in the framework of ultrasound inverse scattering tomography. Those parameters are the speed of sound, density, and absorption whose values are given as the solution of an inhomogeneous Helmholtz wave equation. The separate reconstruction method is mathematically formulated, the integral equations are discretized using the sinc basis functions, and the Newton-Raphson method is adopted as a numerical solver in a measurement configuration where the object is insonified by an incident plane wave over 360° and the scattered field is measured by detectors arranged in a rectangular fashion around it. Two distinct frequencies are used to separate each parameter of three Gaussian objects that are either located at the same position or separately from each other. Computer simulation results show that the separate reconstruction method is able to separately reconstruct the three mechanical parameters. The absorption parameter turns out to be a little difficult to reconstruct as compared with the other two parameters.


## I. Introduction

Most of the work concerned with diffraction or inverse scattering tomographic techniques have modeled the tissue inhomogeneities as fluctuations of only the ultrasonic refractive index or, equivalently, sound speed about its average value [1-4]. A more realistic wave equation is described that considers the variable density and compressibility in [5, 6]. Norton [7] suggested a method for reconstructing separate images of the variations in density and compressibility within a weak scattering tissue sample from near field scattering measurements using only two long, rectangular transducer elements for broadband, plane wave illuminations. Devaney [8] obtained good separate reconstructions of the density and compressibility fluctuations in the noise-free case using the filtered backpropagation algorithm which is valid under the assumption of small or smooth perturbations. The above work falls into the category of the diffraction tomographic approach, which is poor in reconstruction quality and reconstructable contrast range as compared with the inverse scattering tomographic approach adopted in this paper [9, 10, 12].

Berggren *et al.* [11] reconstructed separate images of speed of sound, density, and absorption through the inversion of exact model wave equations using the alternating variable algorithm. Since the object contrast up to which the Newton-Raphson (NR) method is capable of converging to a correct solution is larger than that of the alternating variable algorithm and the former is better in reconstruction quality than the latter [10], it is highly valuable to apply the NR method to obtain the exact inverse scattering solutions of the three intrinsic mechanical parameters of interest. In order to achieve this goal, at least two frequencies must be used to distinguish the frequency-independent speed of sound term from the frequency-dependent density term. The fact that the velocity dispersion in biological tissues is not strong needs to be utilized.

## II. Problem Formulation

The acoustic wave equation for field $f_{\omega\phi}(\vec{r})$, considering the density $\rho(\vec{r})$, is given by

$$\nabla^2 f_{\omega\phi}(\vec{r}) + k_{0\omega}^2 f_{\omega\phi}(\vec{r}) = k_{0\omega}^2 \gamma_{\omega}(\vec{r}) f_{\omega\phi}(\vec{r}) \quad (1)$$

*Daejin University
Manuscript Received : January 21, 1999.

where the complex scattering potential is of the following form [5]:

$$\gamma_\omega(\vec{r}) = \{1 - c_0^2/c(\vec{r}) - j2c_0^2\alpha(\vec{r})/[\omega c(\vec{r})]\} + (c_0^2/\omega^2)\rho^{1/2}(\vec{r})\nabla^2\rho^{-1/2}(\vec{r}) = \gamma_1(\vec{r}) + K_\omega\gamma_2(\vec{r}). \quad (2)$$

Here, $r$ is the field point, $c_0$ is the speed of sound in water, $c(r)$ is the speed of sound in a medium, including water, $j$ is the imaginary number, $\alpha(r)$ is the absorption, $k_\omega$ is the wave number given as $\omega/c_0$, $K_\omega$ is a frequency-dependent scale factor equal to $c_0^2/\omega^2$, and $\omega$ and $\phi$ are, respectively, the angular frequency and propagation direction of a plane wave. In subsequent sections, $\gamma_1(r)$ and $\gamma_2(r)$ will refer to the first and second terms of $\gamma_\omega(r)$, respectively.

Transforming (1) into the equivalent Lippmann-Schwinger integral equation through the use of Green's function method, and applying the method of moments with the sinc basis functions and Dirac delta testing functions, we obtain (3a) at object grid points and (3b) at detector grid points:

$$f_{\omega\phi}(n) = f_{\omega\phi}^{(in)}(n) + \sum_i [\gamma_1(i) + K_\omega\gamma_2(i)] f_{\omega\phi}(i) C_\omega(n;i) \quad (3a)$$

$$f_{\omega\phi}^{(SC)}(m) = \sum_i [\gamma_1(i) + K_\omega\gamma_2(i)] f_{\omega\phi}(i) D_\omega(m;i) \quad (3b)$$

where the superscripts ($in$) and ($sc$) are short for incident and scattered, respectively, and $n$ and $m$ each are indices indicating a point on a two-dimensional grid. Both $C$ and $D$ are coefficients resulting from the use of the sinc basis and impulse testing functions in a two-dimensional Green's function [12]. Equations (3a) and (3b) are called field and detector ones, respectively, since the former is associated with the total field and the latter, the detector field. Transposing the above field and detector equations, we get the following field and detector residual equations (4a) and (4b):

$$r_{\omega\phi}^{(fld)}(n) = f_{\omega\phi}^{(in)}(n) - f_{\omega\phi}(n) + \sum_i [\gamma_1(i) + K_\omega\gamma_2(i)] f_{\omega\phi}(i) C_\omega(n;i) \quad (4a)$$

$$r_{\omega\phi}^{(det)} = f_{\omega\phi}^{(sc)}(m) - \sum_i [\gamma_1(i) + K_\omega\gamma_2(i)] f_{\omega\phi}(i) D_\omega(m;i) \quad (4b)$$

where the two superscripts ($fld$) and (det) stand for field and detector, respectively. The above equations form a nonlinear system of equations which will be solved using the NR method. Taking the first-order Taylor series expansions of both (4a) and (4b) and setting each of them to zero results in the following NR equations:

$$-r_{\omega\phi}^{(fld)}(n) = \sum_i f_{\omega\phi}(i) C_\omega(n;i)[\delta\gamma_1(i) + K_\omega\delta\gamma_2(i)] + \sum_i \{-\delta(i;n) + [\gamma_1(i) + K_\omega\gamma_2(i)] C_\omega(n;i)\} \delta f_{\omega\phi}(i) \quad (5a)$$

$$-r_{\omega\phi}^{(det)}(m) = -\sum_i f_{\omega\phi}(i) D_\omega(m;i)[\delta\gamma_1(i) + K_\omega\delta\gamma_2(i)] - \sum_i [\gamma_1(i) + K_\omega\gamma_2(i)] D_\omega(m;i) \delta f_{\omega\phi}(i) \quad (5b)$$

where $\delta(i;n)$ is the Kronecker delta function, which equals unity if $i=n$ and zero otherwise. In addition, unknowns, $\delta\gamma_1(n)$, $\delta\gamma_2(n)$ and $\delta f_{\omega\phi}(n)$ denote the NR steps for the speed of sound and absorption term in the scattering potential, the density term in the scattering potential, and the total field, respectively. Quantities $\gamma_1(n)$, $\gamma_2(n)$, and $f_{\omega\phi}(n)$ are updated by an amount equal to the NR steps just obtained from both (5a) and (5b), i.e., $\delta\gamma_1(n)$, $\delta\gamma_2(n)$ and $\delta f_{\omega\phi}(n)$, respectively, until there is no further improvement in the iterates.

Now we reconstruct the three ultimate scattering potential constituent parameters, i.e., the speed of sound, density, and absorption, using only two frequencies. Assuming the absorption varies linearly with frequency as $\alpha(n)=\beta(n)\omega$, the scattering potential at an angular frequency $\omega$ can be written as

$$\gamma_\omega(n) = \{1 - [c_0/c(n)]^2 + K_\omega\gamma_2(n)\} - j2c_0^2\beta(n)/c(n). \quad (6)$$

The absorption coefficient $\beta(n)$ can readily be obtained by taking the imaginary part of (6), once the speed of sound $c(n)$ has been determined. We now proceed with the determination of the remaining two parameters, i.e., both the speed of sound and density. Letting $\gamma_{\omega 1}(n)$ and $\gamma_{\omega 2}(n)$ denote the scattering potentials reconstructed using two angular frequencies $\omega_1$ and $\omega_2$, respectively, based on the NR method, we obtain the following system of two linear algebraic equations in two unknowns $[c_0/c(n)]^2$ and $\gamma_2(n)$:

$$\mathrm{Re}[\hat{\gamma}_{\omega_1}(n)] = 1 - [c_0/c(n)]^2 + K\omega_1\gamma_2(n) \quad (7a)$$

$$\mathrm{Re}[\hat{\gamma}_{\omega 2}(n)] = 1 - [c_0/c(n)]^2 + K\omega_2\gamma_2(n). \quad (7b)$$

The set of (7a) and (7b) can be solved for $c(n)$ and $\gamma_2(n)$ to yield the speed of sound term and the density-related term as follows:

$$c(n) = c_0\left\{1 - \frac{\omega_1^2 \mathrm{Re}[\hat{\gamma}_{\omega_1}(n)] - \omega_2^2 \mathrm{Re}[\hat{\gamma}_{\omega_2}(n)]}{\omega_1^2 - \omega_2^2}\right\}^{-1/2} \quad (8)$$

$$\gamma_2(n) = \frac{\mathrm{Re}[\hat{\gamma}_{\omega_1}(n)] - \mathrm{Re}[\hat{\gamma}_{\omega_2}(n)]}{(c_0/\omega_1)^2 - (c_0/\omega_2)^2} \quad . \quad (9)$$

Since the left-hand side of involves the Laplacian, it should be solved again to reconstruct the density itself. Letting $\rho^{-1/2}(n)=u(n)$ , we get

$$\nabla^2 u(n) = u(n)\gamma_2(n) \quad . \quad (10)$$

Taking the finite-difference approximation of the Laplacian operator $\nabla^2$ with the grid spacing $h$ leads to a linear system of equations subject to the boundary condition which requires that $u(n)$ at the detector grid points be unity, since the density of water at those grid points equals unity.

## III. Numerical Results

All computer simulations are performed in single precision arithmetic on a Pentium II 233MHz PC for a square imaging grid of size 32 × 32 pixels on the rectangular periphery of which the ultrasound detectors are positioned. The measurement geometry is shown in Figure 1 where an object immersed in water is irradiated by an incident plane wave whose propagation direction is varied 32 times in equiangle steps over 360° and the scattered field is measured in detectors located on the four sides of the square.

The speed $c_0$ of sound in the homogeneous embedding medium of water is set to 1500 m/s, and the scattered field is obtained by solving (3b). For each of two frequencies $f_1$ = 1 MHz and $f_2$ = 0.9MHz, reconstructions are repeated using the NR method where ten linearizations are done with the number of inner iterations set to 100. The imaging grid is discretized at intervals of one quarter of the wavelength corresponding to the higher frequency $f_1$ = 1MHz; therefore, the pixel widt $h$ in both $x$ and $y$ directions is equal to 0.0375cm. The normalized mean square reconstruction errors in percent, $c_\epsilon$, $\rho_\epsilon$, and $\beta_\epsilon$ for the speed of sound, the density, and the absorption coefficient, respectively, are defined as follows:

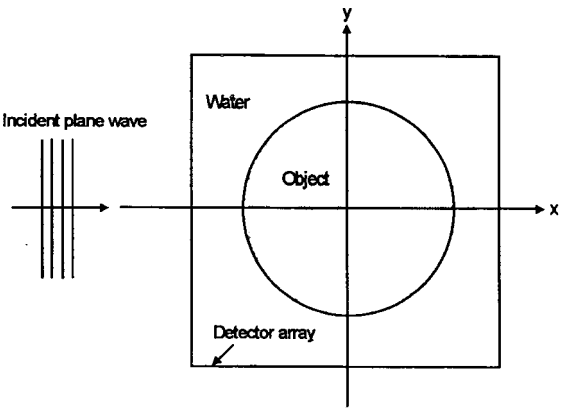


Figure 1. Measurement setup for scattered field where the plane wave is incident upon the scattering object at an angle of 0° with respect to the x axis.

$$c_\epsilon = \left\{\sum_n [c(n) - \hat{c}(n)]^2 / \sum_n c^2(n)\right\}^{1/2} 100\% \quad (11a)$$

$$\rho_\epsilon = \left\{\sum_n [\rho(n) - \hat{\rho}(n)]^2 / \sum_n \rho^2(n)\right\}^{1/2} 100\% \quad (11b)$$

$$\beta_\epsilon = \left\{\sum_n [\beta(n) - \hat{\beta}(n)]^2 / \sum_n \beta^2(n)\right\}^{1/2} 100\% \quad (11c)$$

where $c(n)$, $\rho(n)$, and $\beta(n)$ denote the original speed of sound, density, and absorption coefficients, respectively, and $\hat{c}(n), \hat{\rho}(n)$, and $\hat{\beta}(n)$ denote the reconstructed speed of sound, density, and absorption coefficients, respectively. Three overlapped and separated Gaussian profile objects each are chosen as the scattering objects where the latter are roughly four times as narrow in the region of support as the former. Table 1 lists the reconstruction errors in percent for various combinations of the speed of sound, density, and absorption coefficient. Both object types I and II correspond to the overlapped Gaussian object case, whereas both object types III and IV, the separated Gaussian object case. The parameters $c$, $\rho$, and $\beta$ are, respectively, in units of $10^5$ cm/s, g/cm$^3$, and dB/cm/MHz.

Table 1. Reconstruction errors in percent for various object contrasts.

| Object Type | c | ρ | β | $c_\epsilon$ | $\rho_\epsilon$ | $\beta_\epsilon$ |
|---|---|---|---|---|---|---|
| I | 1.579 | 1.3 | 0.8 | 0.009 | 0.733 | 0.852 |
| II | 1.429 | 1.4 | 0.7 | 0.009 | 0.628 | 0.047 |
| III | 1.667 | 1.3 | 0.8 | 0.070 | 0.593 | 5.971 |
| IV | 1.364 | 2.0 | 2.0 | 0.078 | 0.631 | 6.530 |

The left and right panels in Figure 2 represent isometric plots of the original and reconstructed profiles of the three parameters for the case of object type I, respectively. From top to bottom, the speed of sound, density, and absorption coefficients are displayed in units of cm/s, g/cm$^3$, and in cm$^{-1}$Hz$^{-1}$, respectively. Figure 3 shows the original (square)

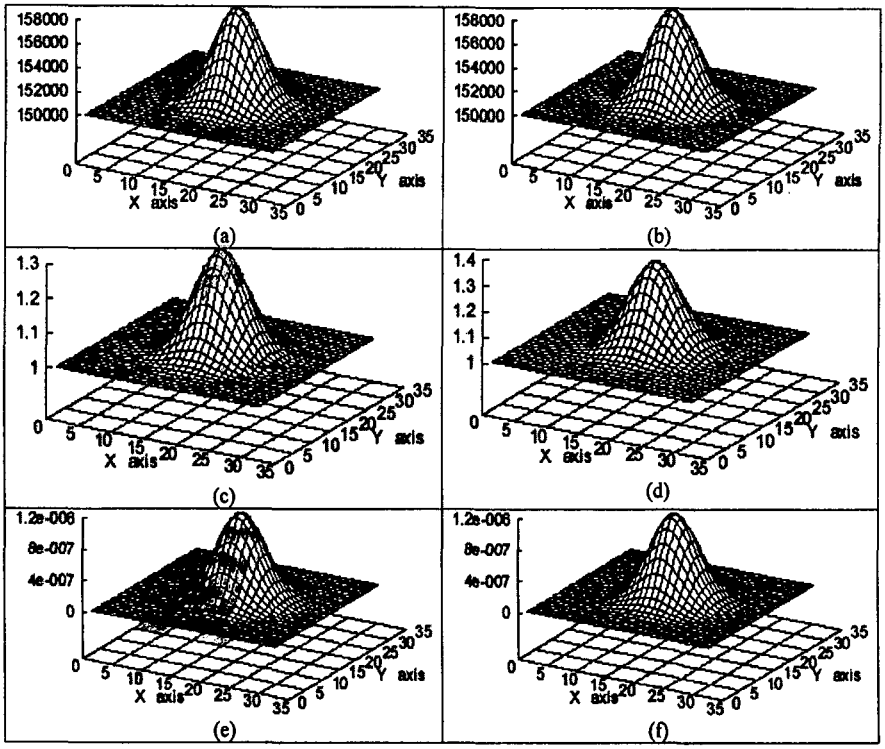


Figure 2. Original (left panels) and reconstructed (right panels) speed of sound, density, and absorption from top to bottom for the case of overlapped profiles.

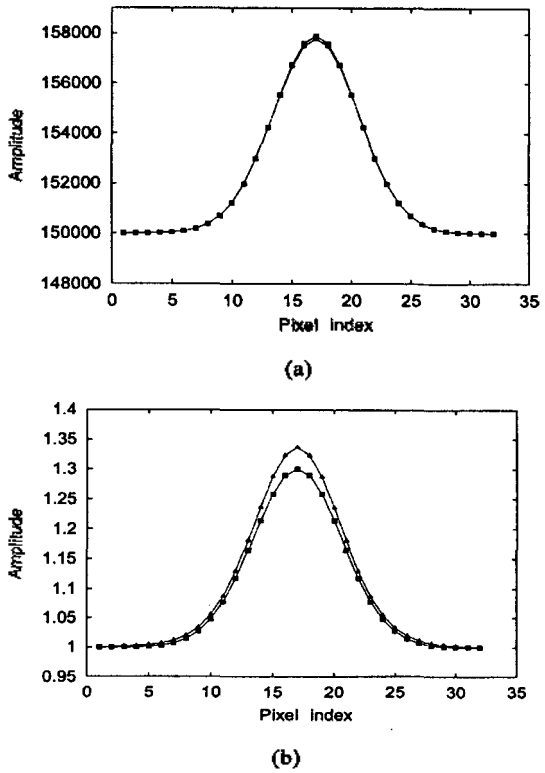


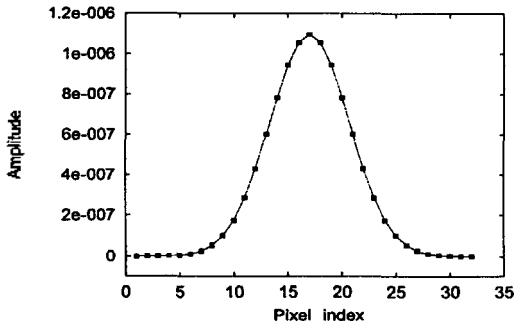


Figure 3. Comparison of the original (square) and reconstructed (triangle) center line profiles of (a) speed of sound, (b) density, and (c) absorption.

and reconstructed (triangle) center line profiles of (a) the speed of sound, (b) density, and (c) absorption coefficients from top to bottom. We can see from the figures that the separate reconstruction method is valid and has good performance.

Numerical simulation results are also presented for the

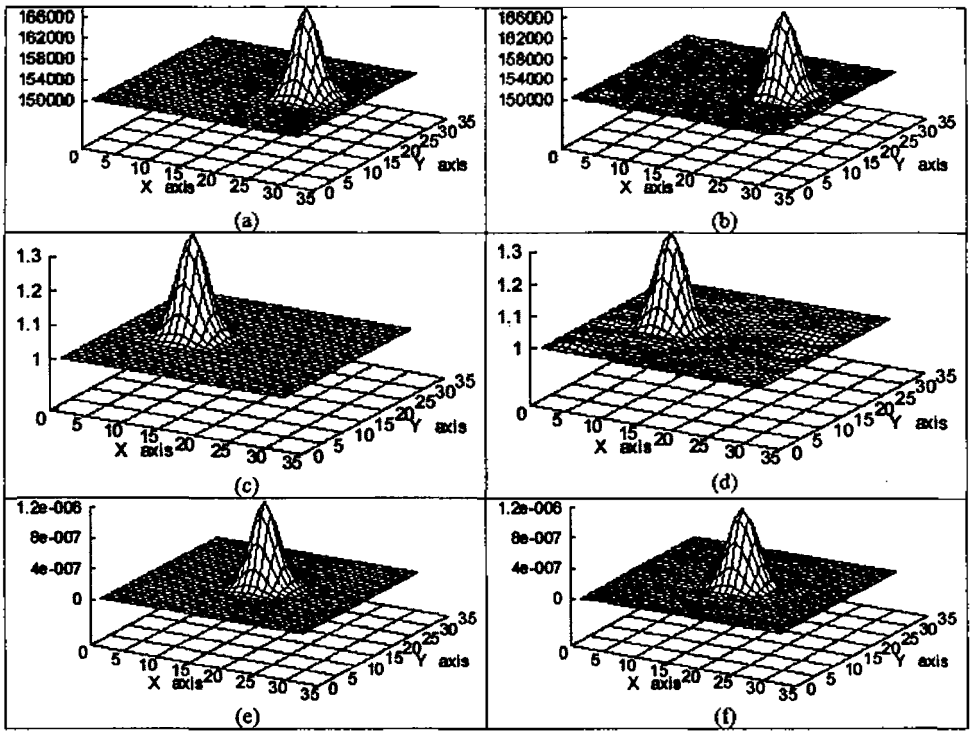


Figure 4. Original (left panels) and reconstructed (right panels) speed of sound, density, and absorption from top to bottom for the case of separated profiles.

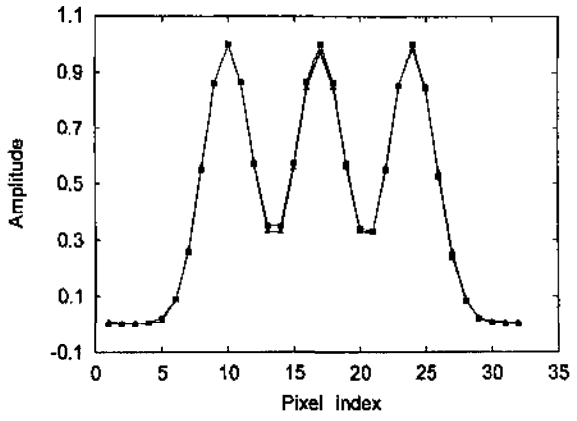


Figure 5. Comparison of the original (square) and reconstructed (triangle) center line profiles of speed of sound (right), density (left), and absorption (middle) where the values are each normalized.

case of object type III. Shown in Figure 4 are isometric plots of the three original (left) and reconstructed (right) parameters. The reconstructed profiles on the right hand side show very small fluctuations in the background. The original (square) and reconstructed (triangle) center line profiles are superimposed together after normalization for the sake of comparison in Figure 5. From left to right, three Gaussian shapes each correspond to the density, absorption, and speed of sound distributions. It can be clearly seen that they match very well.

## IV. Conclusions

In this paper a method of separately reconstructing the speed of sound, density, and absorption with two distinct frequencies is mathematically formulated and solved using the NR method, and its good performance is demonstrated through computer simulations. Two types of Gaussian objects are used as the scattering potential. One is of the overlapped Gaussian type, and the other is of the separately located Gaussian type. The reconstruction quality of the absorption is not as good as that of the speed of sound and density. This is due to the fact that as the absorption increases, the received scattered field decreases. When the object has sharp edges, the density reconstruction shows poor performance, because the Laplacian operation is involved.

### Acknowledgments

Helpful discussions with Dr. W. W. Kim are gratefully acknowledged.

## References


1. C. Lu, J. Lin, W. Chew, and G. Otto, "Image reconstruction with acoustic measurement using distorted Born iterative method," *Ultrason. Imaging 18*, no. 2, pp. 140-156, 1996.
2. O. S. Haddadin and E. S. Ebbini, "Imaging strongly scattering media using a multiple frequency distorted Born iterative method," *IEEE Trans. Ultrason.* Ferroelec. Freq. Contr. **45**, no. 6, pp. 1485-1496, Nov. 1998.
3. O. S. Haddadin, S. D. Lucas, and E. S. Ebbini, "Solution to the inverse scattering problem using a modified distorted Born iterative algorithm," in *Proc. IEEE Ultrason.* Symp. **41**, no. 5, Nov. 1995, pp. 1411-1414.
4. T. J. Cavicchi, S. A. Johnson, and W. D. O' Brien, Jr., "Application of the sinc basis moment method to the reconstruction of infinite circular cylinders," *IEEE Trans.* Ultrason. Ferroelec. Freq. Contr. **35**, no. 1, pp. 22-33, Jan. 1988.
5. S. A. Johnson, F. Stenger, C. Wilcox, J. Ball, and M. J. Berggren, "Wave equations and inverse solutions for soft tissue," Acoustical Imaging **11**, J. P. Powers, Ed. New York, NY: Plenum, 1982, pp. 409-424.
6. P. M. Morse and K. U. Ingard, *Theoretical Acoustics* (McGraw-Hill, New York, 1968).
7. S. J. Norton, "Generation of separate density and compressibility images in tissue," Ultrason. Imaging **5**, no. 3, pp. 240-252, July 1983.
8. A. J. Devaney, "Variable density acoustic tomography," *J. Acoust. Soc. Amer.* **78**, pp. 120-130, July 1986.
9. M. Slaney, A.C. Kak, and L. E. Larsen, "Limitations of imaging with first-order diffraction tomography," *IEEE Trans.* Microwave Theory Tech. **MTT-32**, no. 8, pp. 860-874, Aug. 1984.
10. W. W. Kim, S. A. Johnson, M. J. Berggren, F. Stenger, and C. H. Wilcox, "Analysis of inverse scattering solutions from single frequency, combined transmission and reflection data for the Helmholtz and Riccati exact wave equations," Acoustical Imaging **15**, H. W. Jones, Ed. New York, NY: Plenum, 1986, pp. 359-369.
11. M. J. Berggren, S. A. Johnson, B. L. Carruth, W. W. Kim, F. Stenger, and P. K. Kuhn, "Ultrasound inverse scattering solutions from transmission and/or reflection data," in *Proc. SPIE 671*, Newport Beach, CA, 1986, pp. 114-121.
12. M. L. Tracy and S. A. Johnson, "Inverse scattering solutions by a sinc basis, multiple source, moment method-Part II: Numerical evaluations," *Ultrason. Imaging 5*, no. 4, pp. 376-392, Oct. 1983.



▲Sung-Jae Kwon

Sung-Jae Kwon was born in Taegu, Korea, on August 18, 1961. He received the B. S. degree in electronic engineering from Kyungpook National University in 1984, and the M. S. and Ph. D. degrees in electrical engineering from KAIST in 1986 and 1990, respectively. He worked at LG Electronics Inc. from 1990 to 1997 as a principal engineer. Currently, he teaches in the Department of Communications Engineering, Daejin University in Pochun, Korea. His research interests are in areas of inverse scattering, radar, and DTV. He is a member of the ASK, IEEK, KOSBE, and IEEE.